Intermetallics 16 (2008) 779–784

Contents lists available at ScienceDirect

Intermetallics

journal homepage: www.elsevier.com/locate/intermet

Analysis of element-content effects on equilibrium segregation at γ/γ' interface in Ni-base superalloys using the cluster variation method

T. Kitashima *, T. Yokokawa, A.C. Yeh, H. Harada

High Temperature Materials Center, National Institute for Materials Science, 1-2-1, Sengen, Tsukuba, Ibaraki 305-0047, Japan

ARTICLE INFO

Article history:
Received 6 November 2007
Received in revised form 28 January 2008
Accepted 25 February 2008
Available online 16 April 2008

Keywords:
D. Phase interfaces
E. Phase stability, prediction
B. Order/disorder transformations
D. Site occupancy
G. Aero-engine components

ABSTRACT

Effects of alloying element-content on equilibrium segregation at and adjacent to the (100) γ/γ' interface in Ni-base superalloys were analyzed by using the cluster variation method incorporated with tetrahedron approximation and the phenomenological Lennard–Jones potential. Results suggest that Al-site occupiers in the γ' phase such as Mo, Re and W were enriched near the interface on the side of the γ phase. On the other hand, Co, which prefers to substitute for Ni site, exhibited minimal segregation in the γ phase. The enrichment of the refractory elements such as Mo, Re and W around the interface was moderated, because Co addition slightly diluted refractory elements throughout the γ phase.

1. Introduction

Ni-base single-crystal superalloy is a key material for a high-temperature turbine section in an aero engine. Such Ni-base superalloy is partially creep-strengthened by solid-solution strengthening due to additions of refractory elements such as Mo, Re and W. However, the excessive alloying of these elements promotes precipitation of Topologically Closed-Packed (TCP) phases that degrade Ni-base superalloy's mechanical properties. It has been reported that additions of Co, Ru or Ir can be beneficial in terms of hindering the TCP precipitation [1–5]. This associated underlying mechanism, which may be dependent of the element of Co, Ru and Ir, is controversial although there have been various investigations [1,3,6–9]. One of the possible factors for enhancing the phase stability could be the suppression of equilibrium element segregation at the γ/γ' interface by the addition of Co, Ru or Ir. This might be because that interfacial segregation could induce the nucleation of TCP phases. However, the equilibrium element segregation around the γ/γ' interface has not been previously well-understood.

Many atom probe microanalyses have been conducted on γ/γ' interfacial chemical profile in multi-component Ni-base superalloys, focusing on the local equilibrium at the γ/γ' interface [10–13]. Blavette et al. reported Cr enrichment together with Al depletion in the γ phase close to the interface [10]. Murakami et al. [11] and Warren et al. [12] showed Re enrichment in the γ matrix around the γ/γ' interfaces. However, even atom probe microanalysis has a difficulty identifying crystal structure at the interface because the doped quantities of refractory elements are small, i.e., the associated statistic errors in the measurement are large.

The present study was carried out to provide basic understanding on the effect of element quantities at the (100) γ/γ' interface under the equilibrium state. As for the addition effects of Co, Ru and Ir on the interfacial profile, published thermodynamic data for Ru and Ir, which is necessary for the accurate determination of atomic interactions, are limited. So, only the effect of Co was focused in the present article. In order to clarify the content effects of refractory elements and Co on the interfacial segregation, Ni–Al–Mo, Ni–Al–Co, Ni–Al–Mo–Re–W and Ni–Al–Co–Mo–Re–W systems were investigated using the cluster variation method (CVM).

2. Modeling

In order to model an Inter-Phase Boundary (IPB) of γ/γ' on the (100) plane in a Ni-base superalloy, a supercell shown in Fig. 1 was employed for the initial lattice of calculation. On the left, a disordered γ phase is represented by fcc cubes. The right side shows $L1_2$ structure of an ordered γ' phase with Al sites at the cube corners and Ni sites at the centers of the faces. The alternation of Al-rich planes and Al-depleted planes in the γ' phase can be found. Although only 15 atomic planes which are parallel to the boundary are shown in Fig. 1, the actual supercell used in the calculations consists of 60 planes (29 A1 cubes and 29 $L1_2$ cubes).

* Corresponding author. Tel.: +81 29 859 2428; fax: +81 29 859 2501.
E-mail addresses: kitashima.tomonori@nims.go.jp (T. Kitashima), yokokawa.tadaharu@nims.go.jp (T. Yokokawa), yeh.Anchou@nims.go.jp (A.C. Yeh), harada.hiroshi@nims.go.jp (H. Harada).

0966-9795/$ – see front matter © 2008 Elsevier Ltd. All rights reserved.
doi:10.1016/j.intermet.2008.02.015

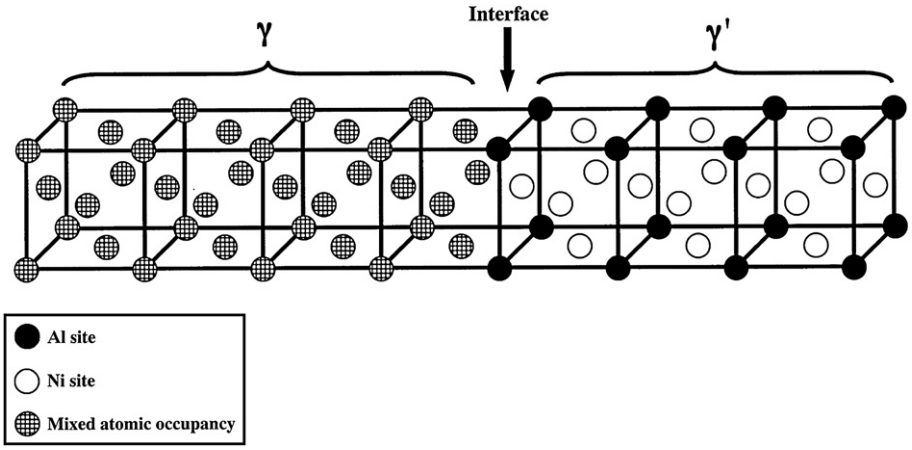

Fig. 1. Supercell with a (100) γ/γ' interface. White and black spheres indicate Ni sites and Al sites in $L1_2$ structure of γ' phase. Meshed spheres indicate mixed atomic occupancies in A1 structure of γ phase.

The atomic interactions in real alloys are considerably more complex than the pair and many-body energies used in the generalized Ising models [14]. However, Sanchez et al. [14] and Enomoto et al. [15–17] have already demonstrated that their CVM incorporated with tetrahedron approximation and phenomenological Lennard–Jones (L–J) potentials provided a reasonably accurate description of equilibrium between γ/γ' phases in the binary and multi-component Ni-base superalloys. In addition, it was demonstrated that their CVM using the L–J potential that the simulated site fractions of alloying elements in a γ' phase were in good agreement with those observed by the atom probe microanalysis and ALCHEMI (Atomic site Location by Channeling Enhanced Microanalysis) [14–16,18–20]. In the present calculations, their L–J potentials [14–17] were employed to obtain the internal energy of the system. In the CVM, the internal energy E is written as [21]

$$E = \frac{1}{2} wN \sum_n \sum_{ij} e_{ij}(r_n) y_n(i,j) \tag{1}$$

where $w = 12$ is the nearest neighbor coordination number in the fcc lattice, N is the total number of lattice points, $y_n(i,j)$ is the nearest neighbor pair probability distribution on 'n'th plane and $e_{ij}(r_n)$ is the pair energy with atomic distance r_n on 'n'th plane obtained by L–J potential as follows [14],

$$e_{ij}(r_n) = e_{ij}^0 \left[\left(\frac{r_{ij}}{r_n} \right)^8 - 2 \left(\frac{r_{ij}}{r_n} \right)^4 \right] \tag{2}$$

The potential parameters e_{ij}^0 and r_{ij} are listed in Table 1, which were reported by Sanchez et al. [14] and Enomoto et al. [15–17] as mentioned above.

Cluster probabilities and entropy expression S in the tetrahedron approximation reported by Kikuchi et al. [21] with an Inter-Phase Boundary (IPB) in the system were applied in this study, assuming that the γ/γ' interface was coherent for simplicity. In order to obtain the most probable atomic configuration under the equilibrium state, the grand potential G of the system defined as $G = E - TS + PV - \sum \mu_i N_i$ was minimized with respect to both $z_n(i,j,k,l)$ and the atomic volume V at constants T, P and μ_i, where T is the temperature, P is the pressure, μ_i is the chemical potential of the 'i'th species, N_i is the total number of the 'i'th species in the entire system including the boundary region, and $z_n(i,j,k,l)$ is the probability of finding atoms (i, j, k, l) on the tetrahedron cluster in the 'n'th plane, under the following continuity constraint (3) and normalization condition (4) [21,22]:

$$y_n(i,j) = \sum_{k,l} z_n(i,j,k,l) = \sum_{k,l} z_{n-1}(k,l,i,j), \tag{3}$$

$$\sum_{i,j,k,l} z_n(i,j,k,l) = 1. \tag{4}$$

In minimizing the G with respect to $z_n(i,j,k,l)$, the following set of equations was solved by the iteration procedure reported by Kooi [22], using Natural Iteration Method (NIM) [23]:

$$z_n(i,j,k,l) = z_n^0(i,j,k,l) \exp\left[\frac{\beta}{2} \lambda_n + \alpha_n(i,j) - \alpha_{n+1}(k,l) \right], \tag{5a}$$

where

$$\begin{aligned} z_n^0(i,j,k,l) = \exp\Big[& -\frac{\beta}{2} \Big\{ e_{ij}(r_n) + e_{ik}(r_n) + e_{il}(r_n) + e_{jk}(r_n) \\ & + e_{jl}(r_n) + e_{kl}(r_n) \Big\} + \frac{\beta}{8} \Big(\mu_i + \mu_j + \mu_k + \mu_l \Big) \Big] \\ & \times \left[y_n(i,j) v_{\mathrm{PPn}}(i,k) v_{\mathrm{PQn}}(i,l) v_{\mathrm{QPn}}(j,k) v_{\mathrm{QQn}}(j,l) y_{n+1}(k,l) \right]^{1/2} \\ & \times \left[x_n(i) u_n(j) x_{n+1}(k) u_{n+1}(l) \right]^{-5/8}. \end{aligned} \tag{5b}$$

Table 1
Lennard–Jones potential parameters used in the present calculations [14–17]

	Ni	Al	Co	Mo	W	Re	
$e_{ij}^0/e_{\mathrm{NiNi}}^0$	1.000	1.000	1.002	1.275	1.560	1.420	Ni
		0.760	0.910	1.035	1.238	1.238	Al
r_{ij}/r_{NiNi}			0.998	1.356	1.509	1.409	Co
Ni	1.000			1.576	1.791	2.091	Mo
Al	1.053	1.149			1.960	1.980	W
Co	1.007	1.009	1.006			2.004	Re
Mo	1.028	1.147	1.062	1.095			
W	1.029	1.150	1.030	1.126	1.132		
Re	1.027	1.150	1.030	1.126	1.102	1.104	

$\mathrm{Ne}_{\mathrm{NiNi}}^0 = 17.13$ kcal/mol, $r_{\mathrm{NiNi}} = 2.491$ Å.